East European Journal of Physics. 2. 4–18 (2026)
DOI: 10.26565/2312-4334-2026-2-01 ISSN 2312-4334

EXPLORING BIANCHI TYPE III UNIVERSE WITH QUADRATIC TRACE OF STRESS-ENERGY TENSOR IN $f(R,T)$ THEORY OF GRAVITY

Chandra Rekha Mahanta, **Kankana Pathak***
Department of Mathematics, Gauhati University, Guwahati - 781014 (INDIA)
*Corresponding Author e-mail: kankanapathak@gauhati.ac.in
Received January 22, 2026; revised March 23, 2026; accepted April 6, 2026

In this work, we consider a spatially homogeneous and anisotropic Bianchi type III universe in $f(R,T)$ gravity with the functional form $f(R,T) = f_1(R) + f_2(T)$ with $f_1(R) = \lambda_1 R$ and $f_2(T) = \lambda_2 T + \lambda_3 T^2$, where λ_1, λ_2 and λ_3 are free parameters. We obtain exact solutions of the gravitational field equations by considering a power-law expansion of a directional scale factor. By keeping a check on the current values of the parameters of cosmological significance such as the Hubble parameter H and the deceleration parameter q, the dynamics and physical characteristics of the model are investigated. We also determine the functional form $f(R,T)$ of our model by evaluating the Ricci scalar R and the trace T of the stress-energy tensor. We find that our model remains anisotropic throughout its evolution and the pressure of the cosmic matter remains negative. The equation of state parameter ω is found to lie in the quintessence regime and therefore our model behaves like quintessence model of dark energy.

Keywords: *Bianchi type III space-time; $f(R,T)$ gravity; Deceleration parameter; Hubble parameter*

PACS: 98.80.-k, 98.80.Jk, 95.36.+x
MSC2020 83C10, 83C15

1. INTRODUCTION

Recent advancements in observational astrophysics have significantly improved our understanding of the universe's large-scale dynamics. One of the key discoveries is the observation of high-redshift Type Ia Supernovae (SN Ia) [1, 2], which provide clear evidence that the universe is expanding at an accelerating rate. These supernovae are crucial in cosmological research because their predictable luminosity enables precise distance measurements, shedding light on the evolution of cosmic expansion over time.

Additionally, the study of Cosmic Microwave Background (CMB) radiation [3–5], the remnant heat from the Big Bang, has offered valuable insights into conditions of the early universe. Observations from missions such as the Wilkinson Microwave Anisotropy Probe (WMAP) [6–9] have delivered detailed maps of temperature variations in the Cosmic Microwave Background, which are instrumental in determining key cosmological parameters and understanding the overall geometry of the universe.

Furthermore, Large Scale Structures (LSS) [10] represents the distribution of galaxies and matter on vast scales which has provided critical information about the growth of cosmic structures under the influence of gravity and dark energy. Complementing this, Baryon Acoustic Oscillations (BAO) [11–13] serve as a standard ruler for measuring cosmic distances, offering additional confirmation of accelerating expansion of the universe.

These diverse observational data points collectively support that the expansion rate of our universe is increasing that challenges the traditional framework of Einstein's General Theory of Relativity (GTR). Since in its original form, GTR cannot fully explain this late time cosmic acceleration. It encouraged the creation of alternate ideas, such as modifications to gravity or the introduction of dark energy. The accelerated expansion remains one of the most intriguing mysteries in modern cosmology, prompting both theoretical and observational efforts to figure out its underlying causes.

Consequently, various efforts have been made to explain the observed acceleration, which can be broadly classified into two main categories: the dark energy approach and the modified gravity approach.

In the first approach, one considers Einstein's theory of General Relativity to be the theory of gravity and modifies the right hand side of the Einstein field equations by supplementing the stress-energy tensor T_{ij} an exotic component with large negative pressure. This can be done because of the fact that the same observational data which reveal the late time cosmic acceleration also exhibit that more than 95% of the total content of the universe is in the form of some yet unknown components of energy and matter, dubbed dark energy and dark matter comprising respectively about 68.3% and 26.8% of the total matter-energy allocation of the universe. The existence of such an unusual component with large negative pressure, called dark energy, is to be considered to counteract the gravitational pressure of the baryonic matter which contributes positive pressure that decelerates the expansion rate of the universe. Many dark energy candidates are proposed in the literature, the most favored one being the cosmological constant Λ introduced by Einstein in his field equations. However, the cosmological constant Λ as a candidate of dark energy suffers from some theoretical challenges such as its constant equation of state parameter $\omega = -1$, fine-tuning, cosmic coincidence problems etc. So dynamically evolving

Cite as: C. R. Mahanta, K. Pathak, East Eur. J. Phys. 2, 4 (2026), https://doi.org/10.26565/2312-4334-2026-2-01

scalar field models of dark energy such as quintessence [14], k-essence [15], tachyon [16], phantom [17], Holographic Dark Energy (HDE) [18–20], Chaplygin gas model [21–23] etc. have been proposed in the literature.

In the second approach, modified gravity models are constructed by modifying the gravitational part of the Einstein-Hilbert action. This can be done as the fundamental concept of General Relativity is the curvature of space-time described by the Ricci scalar R. There are a number of modified gravity models available in the literature, the simplest and the most studied one being the $f(R)$ theory of gravity [24] which is constructed by replacing the Ricci scalar R in the standard Einstein-Hilbert action by some general function $f(R)$ of R. Some other modified theories of gravity employed in the study of rapid expansion of the universe are $f(R,T)$ gravity [25], $f(G)$ gravity [26], $f(T)$ gravity [27], $f(Q)$ gravity [28] etc. The $f(R,T)$ theory of gravity, proposed by Harko *et al.* [25], has received a lot of attention from researchers as this theory takes care of the early time rapid expansion, called inflation, as well as the current cosmic acceleration. In this theory, the gravitational Lagrangian is an arbitrary function of R and T, where R is the Ricci scalar and T is the trace of the stress-energy tensor T_{ij} the dependence of which may be induced from exotic imperfect fluids or quantum effects. In their work, Harko *et al.* derived gravitational field equations from a variational, Einstein-Hilbert type, principle and presented field equations for the following three explicit forms of the function $f(R,T)$: $f(R,T) = R+2f(T)$, $f(R,T) = f_1(R) + f_2(T)$ and $f(R,T) = f_1(R) + f_2(R)f_3(T)$ where $f_1(R)$, $f_2(R)$ are arbitrary functions of R and $f(T)$, $f_2(T)$, $f_3(T)$ are arbitrary functions of T.

They have also derived the equations of motion of test particles by considering the stress-energy tensor to be conserved in $f(R,T)$ theory of gravity and investigated the constraints on the magnitude of extra-acceleration on the precession of the perihelion of Mercury with the Newtonian limits. Soon after, a number of authors considered the $f(R,T)$ theory of gravity and studied various aspects of this theory in different contexts. Houndjo [29] developed a cosmological model using $f(R,T)$ gravity and discussed the transition of the universe from a matter-dominated phase to its current phase with accelerating expansion. Sahoo *et al.* [30] studied the anisotropic Bianchi III cosmological model in $f(R,T)$ gravity. Samanta and Bishi [31] explored astrophysical parameters like look-back time, luminosity distance, and jerk parameter of the Bianchi type III model in $f(R,T)$ gravity with wet dark fluid. Arora *et al.* [32] investigated late-time viscous cosmology in $f(R,T)$ gravity. Many other authors have explored different aspects of cosmology within the framework of $f(R,T)$ gravity. Mahanta *et al.* [33, 34] have studied cosmological models in $f(R,T)$ theory of gravity. Most of these studies are conducted in a spatially homogeneous and anisotropic background. This is because, although the current universe appears homogeneous and isotropic on a large scale, recent data from the Cosmic Microwave Background (CMB) and observations of large-scale structures support the idea that the universe was once anisotropic before evolving into its current isotropic state.

In this work, we investigate a spatially homogeneous and anisotropic Bianchi type III cosmological model within the framework of $f(R,T)$ gravity, using the functional form $f(R,T) = f_1(R) + f_2(T)$, where $f_1(R) = \lambda_1 R$ and $f_2(T) = \lambda_2 T + \lambda_3 T^2$. Here, λ_1, λ_2, and λ_3 are free parameters. The paper is organized as follows: In section 2, we present the gravitational field equations for this functional form using the metric formalism, assuming the matter source as a perfect fluid. In section 3, we derive the corresponding field equations for the Bianchi type III metric. In section 4, we obtain exact solutions to these field equations by assuming a power-law expansion in a specific spatial direction. In section 5, we explore the physical characteristics and dynamics of the constructed model by examining the evolution of several cosmologically significant physical parameters. In section 6, we discuss about the functional $f(R,T)$ of our model. Finally, we summarize our results with a brief discussion in section 7.

2. Gravitational field equations for the functional form $f(R,T) = f_1(R) + f_2(T)$

The action for $f(R,T)$ theory of gravity proposed by Harko *et al.* is

$$S = \frac{1}{16\pi}\int f(R,T)\sqrt{-g}\; d^4x + \int L_m\sqrt{-g}\; d^4x \tag{1}$$

where $f(R,T)$ is an arbitrary function of Ricci scalar R and the trace $T = g^{ij}T_{ij}$ of stress-energy tensor, each choice of which would generate a specific set of field equations and L_m is the matter Lagrangian density. The stress-energy tensor of matter is defined by

$$T_{ij} = \frac{-2}{\sqrt{-g}}\frac{\delta(\sqrt{-g}L_m)}{\delta g^{ij}} \tag{2}$$

Assuming L_m to depend only on the metric tensor components g_{ij} and not on its derivatives, T_{ij} is obtained as

$$T_{ij} = g_{ij}L_m - 2\frac{\partial L_m}{\partial g^{ij}} \tag{3}$$

Now taking variation of the action Eq.(1) with respect to the metric tensor components g^{ij}, the field equations of $f(R,T)$ gravity are obtained as

$$f_R(R,T)R_{ij} - \frac{1}{2}f(R,T)g_{ij} + (g_{ij}\Box - \bigtriangledown_i\bigtriangledown_j)f_R(R,T) = 8\pi T_{ij} - f_T(R,T)T_{ij} - f_T(R,T)\Theta_{ij} \tag{4}$$

where, $f_R(R,T) = \frac{\partial f(R,T)}{\partial R}$, $f_T(R,T) = \frac{\partial f(R,T)}{\partial T}$, $\Box = \bigtriangledown_i \bigtriangledown^i$, $\bigtriangledown_i$ being the covariant derivative with respect to the symmetric connection Γ associated to the metric g and

$$\Theta_{ij} = -2T_{ij} + g_{ij}L_m - 2g^{lk}\frac{\partial^2 L_m}{\partial g^{ij}\partial g^{lk}} \tag{5}$$

Considering the functional form

$$f(R,T) = f_1(R) + f_2(T) \tag{6}$$

where $f_1(R)$ and $f_2(T)$ are arbitrary functions of R and T respectively, the gravitational field equations from Eq.(4) are obtained as

$$f_1{}'(R)R_{ij} - \frac{1}{2}f_1(R)g_{ij} + (g_{ij}\Box - \bigtriangledown_i\bigtriangledown_j)f_1{}'(R) = 8\pi T_{ij} - f_2{}'(T)T_{ij} - f_2{}'(T)\Theta_{ij} + \frac{1}{2}f_2(T)g_{ij} \tag{7}$$

where the prime denotes differentiation with respect to the argument. For a perfect fluid described by an energy density ρ and pressure p, the stress-energy tensor T_{ij} is given by

$$T_{ij} = (\rho + p)u_i u_j - pg_{ij} \tag{8}$$

where u^i is the four velocity satisfying the conditions

$$u^i \bigtriangledown_j u_i = 0, \quad u_i u^i = 1 \tag{9}$$

The trace T of T_{ij} is therefore given by

$$T = \rho - 3p \tag{10}$$

Taking the matter Lagrangian to be $L_m = -p$, from Eq. (5), Θ_{ij} is obtained as

$$\Theta_{ij} = -2T_{ij} - pg_{ij} \tag{11}$$

Thus, if the matter source is a perfect fluid then the field equations of $f(R,T)$ gravity for the choice Eq.(6) become

$$f_1{}'(R)R_{ij} - \frac{1}{2}f_1(R)g_{ij} = 8\pi T_{ij} + f_2{}'(T)T_{ij} + \left[f_2{}'(T)p + \frac{1}{2}f_2(T)\right]g_{ij} \tag{12}$$

In particular, for $f_1(R) = \lambda_1 R$ and $f_2(T) = \lambda_2 T + \lambda_3 T^2$, where λ_1, λ_2 and λ_3 are free parameters, the Eq.(12) reduces to

$$R_{ij} - \frac{1}{2}Rg_{ij} = \frac{1}{\lambda_1}\left[(8\pi + \lambda_2 + 2\lambda_3 T)\,T_{ij} + \left(p(\lambda_2 + 2\lambda_3 T) + \frac{1}{2}(\lambda_2 T + \lambda_3 T^2)\right)g_{ij}\right] \tag{13}$$

3. THE METRIC AND FIELD EQUATIONS

We consider the spatially homogeneous and anisotropic Bianchi type III metric in the form

$$ds^2 = dt^2 - A^2dx^2 - B^2e^{-2lx}dy^2 - C^2dz^2 \tag{14}$$

where A, B and C are functions of cosmic time t alone and l is a constant. Using comoving coordinates, the field equations (13) for the metric (14) take the form

$$\frac{\ddot{B}}{B} + \frac{\ddot{C}}{C} + \frac{\dot{B}}{B}\frac{\dot{C}}{C} = \frac{1}{\lambda_1}\left[-\left(8\pi + \frac{3}{2}\lambda_2\right)p + \frac{1}{2}\lambda_2\rho + \frac{9}{2}\lambda_3 p^2 + \frac{1}{2}\lambda_3\rho^2 - 3\lambda_3 p\rho\right] \tag{15}$$

$$\frac{\ddot{C}}{C} + \frac{\ddot{A}}{A} + \frac{\dot{C}}{C}\frac{\dot{A}}{A} = \frac{1}{\lambda_1}\left[-\left(8\pi + \frac{3}{2}\lambda_2\right)p + \frac{1}{2}\lambda_2\rho + \frac{9}{2}\lambda_3 p^2 + \frac{1}{2}\lambda_3\rho^2 - 3\lambda_3 p\rho\right] \tag{16}$$

$$\frac{\ddot{A}}{A} + \frac{\ddot{B}}{B} + \frac{\dot{A}}{A}\frac{\dot{B}}{B} - \frac{l^2}{A^2} = \frac{1}{\lambda_1}\left[-\left(8\pi + \frac{3}{2}\lambda_2\right)p + \frac{1}{2}\lambda_2\rho + \frac{9}{2}\lambda_3 p^2 + \frac{1}{2}\lambda_3\rho^2 - 3\lambda_3 p\rho\right] \tag{17}$$

$$\frac{\dot{A}}{A}\frac{\dot{B}}{B} + \frac{\dot{B}}{B}\frac{\dot{C}}{C} + \frac{\dot{C}}{C}\frac{\dot{A}}{A} - \frac{l^2}{A^2} = \frac{1}{\lambda_1}\left[\left(8\pi + \frac{3}{2}\lambda_2\right)\rho - \frac{1}{2}\lambda_2 p + \frac{5}{2}\lambda_3\rho^2 - \frac{3}{2}\lambda_3 p^2 - 7\lambda_3 p\rho\right] \tag{18}$$

$$\frac{\dot{A}}{A} - \frac{\dot{B}}{B} = 0 \tag{19}$$

where an overhead dot denotes differentiation w.r.t. t. Integrating Eq.(19), we get

$$A = mB \tag{20}$$

where m is a constant of integration.

Hence, the field equations (15)-(18) reduce to

$$\frac{\ddot{A}}{A} + \frac{\ddot{C}}{C} + \frac{\dot{A}}{A}\frac{\dot{C}}{C} = \frac{1}{\lambda_1}\left[-\left(8\pi + \frac{3}{2}\lambda_2\right)p + \frac{1}{2}\lambda_2\rho + \frac{9}{2}\lambda_3 p^2 + \frac{1}{2}\lambda_3\rho^2 - 3\lambda_3 p\rho\right] \tag{21}$$

$$2\frac{\ddot{A}}{A} + \left(\frac{\dot{A}}{A}\right)^2 - \frac{l^2}{A^2} = \frac{1}{\lambda_1}\left[-\left(8\pi + \frac{3}{2}\lambda_2\right)p + \frac{1}{2}\lambda_2\rho + \frac{9}{2}\lambda_3 p^2 + \frac{1}{2}\lambda_3\rho^2 - 3\lambda_3 p\rho\right] \tag{22}$$

$$\left(\frac{\dot{A}}{A}\right)^2 + 2\frac{\dot{C}}{C}\frac{\dot{A}}{A} - \frac{l^2}{A^2} = \frac{1}{\lambda_1}\left[\left(8\pi + \frac{3}{2}\lambda_2\right)\rho - \frac{1}{2}\lambda_2 p + \frac{5}{2}\lambda_3\rho^2 - \frac{3}{2}\lambda_3 p^2 - 7\lambda_3 p\rho\right] \tag{23}$$

4. EXACT SOLUTION OF THE FIELD EQUATIONS

From equations (21) and (22), we have

$$\frac{\ddot{A}}{A} + \left(\frac{\dot{A}}{A}\right)^2 - \frac{\ddot{C}}{C} - \frac{\dot{C}}{C}\frac{\dot{A}}{A} - \frac{l^2}{A^2} = 0 \tag{24}$$

Eq.(24) contains two unknowns A and C. Further, we have three field equations in four unknowns A, C, ρ and p. To derive an exact solution and develop a physically realistic model, we adopt a power-law expansion of the form:

$$C = C_0 t^\beta \tag{25}$$

where β and C_0 are positive constants in accordance with the observational findings of an expanding universe [30, 35, 36]. Using Eq.(25) in Eq.(24) and then solving, we obtain

$$A^2 = \frac{l^2 t^2}{1-\beta^2} + C_0^2 k_1 t^{2\beta} + \frac{2l^2 k_2 t^{1-\beta}}{C_0(1-3\beta)} \tag{26}$$

where k_1 and k_2 are constants of integration. Using Eq.(20), we then obtain

$$B^2 = \frac{1}{m^2}\left(\frac{l^2 t^2}{1-\beta^2} + C_0^2 k_1 t^{2\beta} + \frac{2l^2 k_2 t^{1-\beta}}{C_0(1-3\beta)}\right) \tag{27}$$

In this work, we choose $k_2 = 0$ and $0 < \beta < 1$. Then from equations (26) and (27), we get

$$A^2 = \frac{l^2 t^2}{1-\beta^2} + C_0^2 k_1 t^{2\beta} \tag{28}$$

and

$$B^2 = \frac{1}{m^2}\left(\frac{l^2 t^2}{1-\beta^2} + C_0^2 k_1 t^{2\beta}\right) \tag{29}$$

Therefore, the line element (14) becomes

$$ds^2 = dt^2 - \left(\frac{l^2 t^2}{1-\beta^2} + C_0^2 k_1 t^{2\beta}\right)\left(dx^2 + \frac{e^{-2lx}}{m^2}dy^2\right) - C_0^2 t^{2\beta} dz^2 \tag{30}$$

5. DYNAMICS AND PHYSICAL CHARACTERISTICS OF THE MODEL

In this section, we look forward to study the dynamics and physical characteristics of the constructed model. So, we first obtain the expressions for some important parameters of the model and then investigate their behavior as the universe evolves.

5.1. Physical parameters of the model

For our model, the spatial volume is

$$V = a^3 = ABC = \frac{C_0}{m}\left[\frac{l^2 t^{\beta+2}}{1-\beta^2} + C_0^2 k_1 t^{3\beta}\right] \tag{31}$$

The directional Hubble parameters corresponding to our model are

$$H_1 = \frac{\dot{A}}{A} = \frac{\frac{l^2 t}{1-\beta^2} + C_0^2 k_1 \beta t^{2\beta-1}}{\frac{l^2 t^2}{1-\beta^2} + C_0^2 k_1 t^{2\beta}} \tag{32}$$

$$H_2 = \frac{\dot{B}}{B} = \frac{\frac{l^2 t}{1-\beta^2} + C_0^2 k_1 \beta t^{2\beta-1}}{\frac{l^2 t^2}{1-\beta^2} + C_0^2 k_1 t^{2\beta}} \tag{33}$$

$$H_3 = \frac{\dot{C}}{C} = \frac{\beta}{t} \tag{34}$$

The average Hubble parameter is therefore

$$H = \frac{1}{3}(H_1 + H_2 + H_3) = \frac{1}{3}\left[\frac{\frac{2l^2 t}{1-\beta^2} + 2C_0^2 k_1 \beta t^{2\beta-1}}{\frac{l^2 t^2}{1-\beta^2} + C_0^2 k_1 t^{2\beta}} + \frac{\beta}{t}\right] \tag{35}$$

The deceleration parameter is

$$q = -1 + \frac{d}{dt}\left(\frac{1}{H}\right) = -1 - \frac{3\left[\frac{-(\beta+2)l^4 t^4}{(1-\beta^2)^2} + \frac{2l^2 C_0^2 k_1 (2\beta^2-6\beta+1) t^{2\beta+2}}{1-\beta^2} - 3C_0^4 k_1^2 \beta t^{4\beta}\right]}{\left(\frac{l^2(\beta+2)t^2}{1-\beta^2} + 3C_0^2 k_1 \beta t^{2\beta}\right)^2} \tag{36}$$

The expansion scalar is

$$\theta = 3H = H_1 + H_2 + H_3 = \frac{\frac{2l^2 t}{1-\beta^2} + 2C_0^2 k_1 \beta t^{2\beta-1}}{\frac{l^2 t^2}{1-\beta^2} + C_0^2 k_1 t^{2\beta}} + \frac{\beta}{t} \tag{37}$$

The mean anisotropy parameter is

$$\begin{aligned} A_m &= \frac{1}{3}\Sigma_{i=1}^{3}\left(\frac{H_i - H}{H}\right)^2 \\ &= 2 - \frac{3\left(\frac{\frac{l^2 t}{1-\beta^2} + C_0^2 k_1 \beta t^{2\beta-1}}{\frac{l^2 t^2}{1-\beta^2} + C_0^2 k_1 t^{2\beta}}\right)}{\frac{\frac{2l^2 t}{1-\beta^2} + 2C_0^2 k_1 \beta t^{2\beta-1}}{\frac{l^2 t^2}{1-\beta^2} + C_0^2 k_1 t^{2\beta}} + \frac{\beta}{t}} - \frac{9\left(\frac{\frac{l^2 \beta}{1-\beta^2} + C_0^2 k_1 \beta^2 t^{2\beta-2}}{\frac{l^2 t^2}{1-\beta^2} + C_0^2 k_1 t^{2\beta}}\right)}{\left(\frac{\frac{2l^2 t}{1-\beta^2} + 2C_0^2 k_1 \beta t^{2\beta-1}}{\frac{l^2 t^2}{1-\beta^2} + C_0^2 k_1 t^{2\beta}} + \frac{\beta}{t}\right)^2} \end{aligned} \tag{38}$$

And, the shear scalar is

$$\sigma^2 = \frac{1}{3}\left[\frac{\frac{l^2 t}{1-\beta^2} + C_0^2 k_1 \beta t^{2\beta-1}}{\frac{l^2 t^2}{1-\beta^2} + C_0^2 k_1 t^{2\beta}} - \frac{\beta}{t}\right]^2 \tag{39}$$

5.2. Evolution of the physical parameters

From figure 1, we see that as cosmic time t increases, the volume V grows for different values of the parameter β. This indicates an expanding universe, consistent with observations of cosmic expansion. The increase in volume with time supports the idea of a universe evolving from a smaller, denser state (e.g., near a Big Bang-type singularity) towards a more expansive state. The parameter β likely controls the rate of expansion, possibly linked to anisotropic stresses, matter content, or modified gravity effects in the $f(R,T)$ framework. For larger values of β, the rate of expansion might differ, reflecting the influence of β on the model's dynamics.

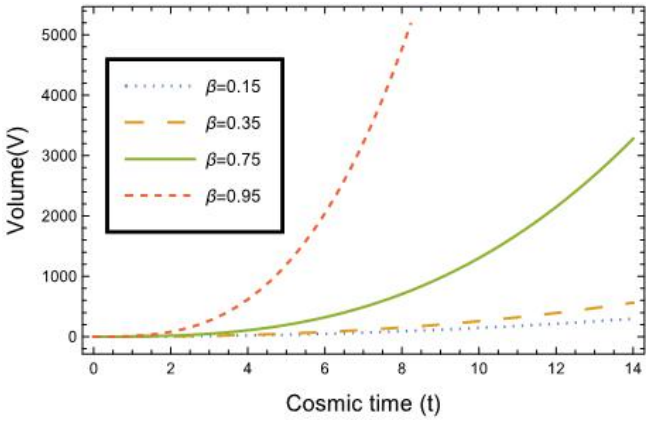

Figure 1. Variation of volume V v/s cosmic time t for different values of β

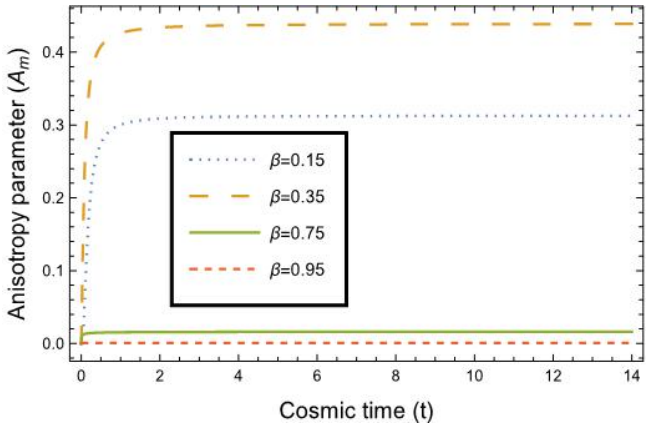

Figure 2. Variation of anisotropy parameter A_m v/s cosmic time t for different values of β

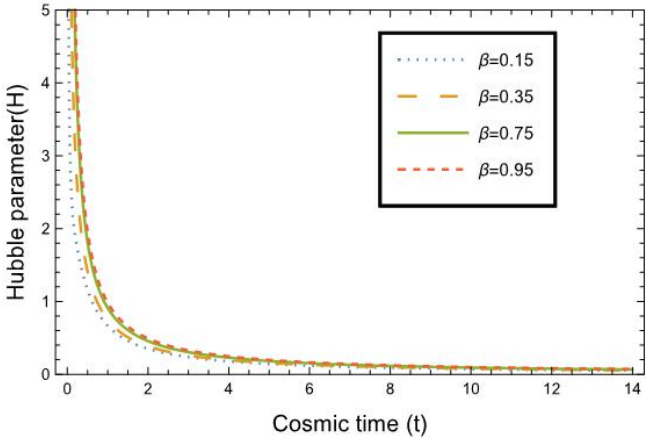

Figure 3. Variation of the average Hubble parameter H v/s cosmic time t for different values of β.

Anisotropy describes the directional variation in the properties of the universe, where the expansion rate differs along various directions. It is quantified by parameters that indicate deviations from isotropy in the metric or the energy-momentum tensor. From figure 2, it is evident that the model retains its anisotropic nature throughout its evolution, implying that the universe does not become perfectly isotropic even at late times. This points to the influence of factors that sustain the directional dependence of the expansion.

In figure 3, we analyze the behavior of the average Hubble parameter (H) as a function of cosmic time t for different values of β viz. $\beta = 0.15$, $\beta = 0.35$, $\beta = 0.75$ and $\beta = 0.95$. The plot reveals that H consistently decreases with increasing cosmic time t, indicating a slowing rate of expansion as the universe evolves. At late times, H asymptotically approaches a constant value, suggesting that the expansion rate stabilizes in the distant future. The variation in β influences the rate at which H decreases, but the overall trend of convergence to a constant value remains the same for all considered

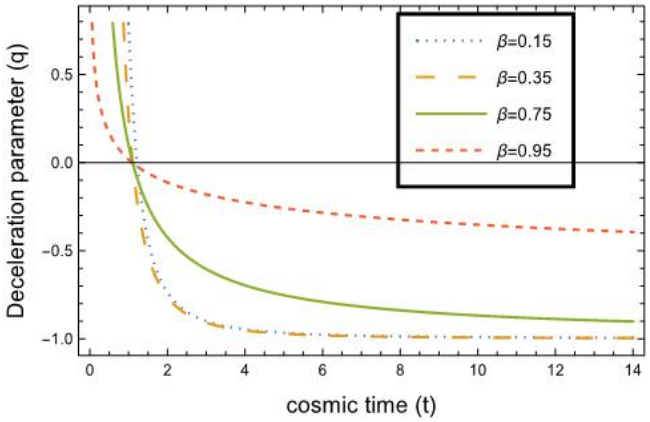

Figure 4. Variation of deceleration parameter q v/s cosmic time t for different values of β

cases. This behavior aligns with the expectation of a universe transitioning toward a steady-state expansion phase.

Figure 4 illustrates the evolution of the deceleration parameter (q) over cosmic time t, highlighting key transitions in the universe's expansion dynamics. The plot clearly shows that the model transitions from an initial decelerating phase ($q > 0$) to the present accelerating phase ($q < 0$), consistent with observational evidence. Furthermore, as cosmic time t progresses toward infinity, the deceleration parameter asymptotically approaches $q \to -1$. This behavior indicates that the universe evolves toward a state of exponential expansion, characteristic of a de Sitter phase dominated by dark energy or a similar cosmological constant-like component.

From the above figures, we find the value $\beta = 0.75$ to be more suitable for our study. So, we stick to this value of β to carry out further studies. Also, we choose $l = 1$, $m = 1$, $C_0 = 1$, $k_1 = 0.1$, $\lambda_1 = -0.1$, $\lambda_2 = 0.2$, $\lambda_3 = 0.3$ for all the plots.

5.3. Jerk parameter

The jerk parameter (j) plays a vital role in cosmology as it provides deeper insights into the dynamics of expansion of the universe. In essence, it provides insights into whether the acceleration itself is speeding up or slowing down over time. The jerk parameter j represents the third derivative of the scale factor $a(t)$ with respect to cosmic time t, normalized in a dimensionless form. It quantifies the rate at which the acceleration of the universe's expansion is changing. The jerk parameter extends the deceleration parameter (q) in a more straightforward way.

A positive jerk indicates that the acceleration is increasing, suggesting a scenario of rapid, ever-accelerating expansion. Conversely, a negative jerk implies that the acceleration is tapering off, hinting at a possible stabilization or deceleration of the expansion in the future. Cosmologists may verify and enhance dark energy and modified gravity models by examining the jerk parameter which helps to uncover whether the current accelerated expansion is driven by a cosmological constant Λ, dynamic dark energy, or other phenomena. This makes it an essential tool for comprehending the universe's past as well as its possible future.

For our model, the jerk parameter $j(t)$ is obtained as

$$
\begin{aligned}
j(t) &= \frac{a^2}{\dot{a}^3}\frac{d^3a}{dt^3} \\
&= 1 + 9\frac{-\frac{(\beta+2)l^4t^2}{(1-\beta^2)^2} + \frac{2C_0^2k_1l^2(2\beta^2-6\beta+1)t^{2\beta}}{(1-\beta^2)} - 3C_0^4k_1^2\beta t^{4\beta-2}}{\left(\frac{(\beta+2)l^2t}{1-\beta^2} + 3C_0^2k_1\beta t^{2\beta-1}\right)^2} \\
&\quad + \frac{9}{\left(\frac{(\beta+2)l^2t}{1-\beta^2} + 3C_0^2k_1\beta t^{2\beta-1}\right)^3 t^3}\left[2t^3\left(\frac{2l^2t}{1-\beta^2} + 2C_0^2k_1\beta t^{2\beta-1}\right)^3\right. \\
&\quad - 3t^3\left(\frac{2l^2}{1-\beta^2} + 2C_0^2k_1\beta(2\beta-1)t^{2\beta-2}\right)\left(\frac{2l^2t}{1-\beta^2} + 2C_0^2k_1\beta t^{2\beta-1}\right)\left(\frac{l^2t^2}{1-\beta^2} + C_0^2k_1t^{2\beta}\right) \\
&\quad \left. + C_0^2k_1\beta(2\beta-1)(2\beta-2)t^{2\beta}\left(\frac{l^2t^2}{1-\beta^2} + C_0^2k_1t^{2\beta}\right)^2 + 2\beta\left(\frac{l^2t^2}{1-\beta^2} + C_0^2k_1t^{2\beta}\right)^3\right]
\end{aligned}
\tag{40}
$$

Figure 5 demonstrates the evolution of the jerk parameter j with respect to cosmic time t. The plot indicates that j decreases as t increases, suggesting a gradual change in the dynamical properties of the universe's expansion. Throughout

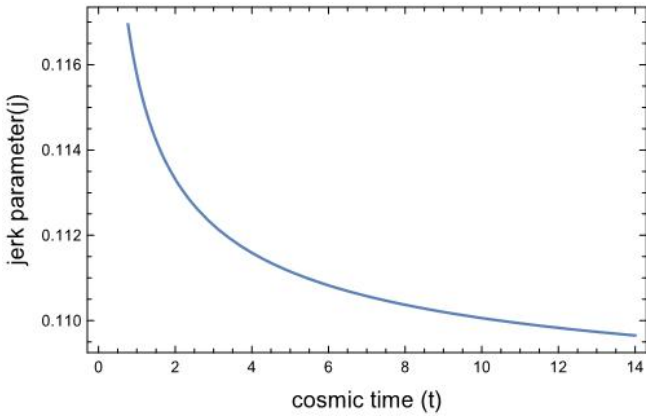

Figure 5. Graph of jerk parameter v/s cosmic time t for $\beta = 0.75$

the evolution, the values of j remain consistently less than 1, which is a key characteristic of cosmological models dominated by quintessence type dark energy.

It is well known that quintessence is a form of dynamic dark energy where the Equation of State parameter ω lies in the range $-1 < \omega < -\frac{1}{3}$, distinguishing it from a cosmological constant ($\omega = -1$). The behavior of the jerk parameter in this model aligns with this description, indicating that the driving force behind the universe's accelerated expansion is not a static cosmological constant but a time varying dark energy component. Thus, the evolution of j in our model provides strong evidence for a quintessence like scenario, where the dynamics of dark energy play a critical role in shaping the universe's expansion history.

5.4. Statefinder diagnostic

The statefinder pair $\{r, s\}$ is defined [37] as

$$r = \frac{1}{aH^3}\frac{d^3a}{dt^3}, \quad s = \frac{r-1}{3(q-\frac{1}{2})} \tag{41}$$

The pair $\{r, s\}$ is a significant geometrical diagnostic tool which can be employed to distinguish different dark energy models such as ΛCDM, Quintessence scalar field model, Holographic dark energy model, Chaplygin gas model etc. ΛCDM model corresponds to the pair $\{1, 0\}$ while the Holographic dark energy model corresponds to $\{1, \frac{2}{3}\}$. The quintessence corresponds to ($r < 1$, $s > 0$) and the Chaplygin gas model corresponds to ($r > 1$, $s < 0$).

For our model, the statefinder pair $\{r, s\}$ is obtained as

$$\begin{aligned}
r &= 1 + 3\frac{\dot{H}}{H^2} + \frac{\ddot{H}}{H^3} \\
&= 1 + 9\frac{-\frac{(\beta+2)l^4t^2}{(1-\beta^2)^2} + \frac{2C_0^2k_1l^2(2\beta^2-6\beta+1)t^{2\beta}}{(1-\beta^2)} - 3C_0^4k_1^2\beta t^{4\beta-2}}{\left(\frac{(\beta+2)l^2t}{1-\beta^2} + 3C_0^2k_1\beta t^{2\beta-1}\right)^2} \\
&\quad + \frac{9}{\left(\frac{(\beta+2)l^2t}{1-\beta^2} + 3C_0^2k_1\beta t^{2\beta-1}\right)^3 t^3}\left[2t^3\left(\frac{2l^2t}{1-\beta^2} + 2C_0^2k_1\beta t^{2\beta-1}\right)^3\right. \\
&\quad - 3t^3\left(\frac{2l^2}{1-\beta^2} + 2C_0^2k_1\beta(2\beta-1)t^{2\beta-2}\right)\left(\frac{2l^2t}{1-\beta^2} + 2C_0^2k_1\beta t^{2\beta-1}\right)\left(\frac{l^2t^2}{1-\beta^2} + C_0^2k_1t^{2\beta}\right) \\
&\quad + C_0^2k_1\beta(2\beta-1)(2\beta-2)t^{2\beta}\left(\frac{l^2t^2}{1-\beta^2} + C_0^2k_1t^{2\beta}\right)^2 \\
&\quad \left. + 2\beta\left(\frac{l^2t^2}{1-\beta^2} + C_0^2k_1t^{2\beta}\right)^3\right]
\end{aligned} \tag{42}$$

$$
\begin{aligned}
s &= \frac{r-1}{3\left(q-\frac{1}{2}\right)} \\
&= \frac{1}{3\left(-\frac{3\left(\frac{-(\beta+2)l^4t^4}{(1-\beta^2)^2}+\frac{2l^2C_0^2k_1(2\beta^2-6\beta+1)t^{2\beta+2}}{1-\beta^2}-3C_0^4k_1^2\beta t^{4\beta}\right)}{\left(\frac{l^2(\beta+2)t^2}{1-\beta^2}+3C_0^2k_1\beta t^{2\beta}\right)^2}-1.5\right)} \\
&\left[9\frac{-\frac{(\beta+2)l^4t^2}{(1-\beta^2)^2}+\frac{2C_0^2k_1l^2(2\beta^2-6\beta+1)t^{2\beta}}{(1-\beta^2)}-3C_0^4k_1^2\beta t^{4\beta-2}}{\left(\frac{(\beta+2)l^2t}{1-\beta^2}+3C_0^2k_1\beta t^{2\beta-1}\right)^2}\right. \\
&\quad +\frac{9}{\left(\frac{(\beta+2)l^2t}{1-\beta^2}+3C_0^2k_1\beta t^{2\beta-1}\right)^3t^3}\left\{2t^3\left(\frac{2l^2t}{1-\beta^2}+2C_0^2k_1\beta t^{2\beta-1}\right)^3\right. \\
&\quad -3t^3\left(\frac{2l^2}{1-\beta^2}+2C_0^2k_1\beta(2\beta-1)t^{2\beta-2}\right)\left(\frac{2l^2t}{1-\beta^2}+2C_0^2k_1\beta t^{2\beta-1}\right)\left(\frac{l^2t^2}{1-\beta^2}+C_0^2k_1t^{2\beta}\right) \\
&\quad \left.\left.+C_0^2k_1\beta(2\beta-1)(2\beta-2)t^{2\beta}\left(\frac{l^2t^2}{1-\beta^2}+C_0^2k_1t^{2\beta}\right)^2+2\beta\left(\frac{l^2t^2}{1-\beta^2}+C_0^2k_1t^{2\beta}\right)^3\right\}\right]
\end{aligned}
\tag{43}
$$

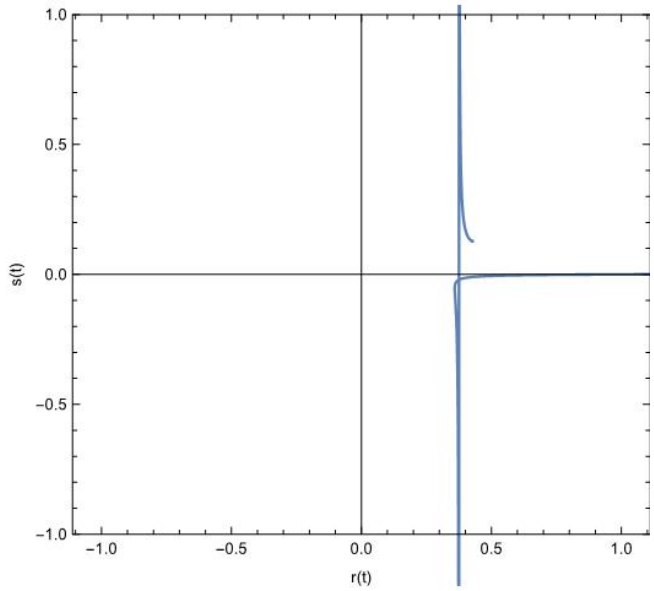

Figure 6. Statefinder pair $r-s$

The model's trajectory in figure 6 suggests that it will continue to exhibit quintessence like behavior in the future, maintaining this specific dynamical profile.

5.5. Evolution of energy density and pressure

In terms of directional Hubble parameters, the field equations (15)-(18) reduce to

$$H_1^2+2H_1H_3-\frac{l^2}{A^2}=\frac{1}{\lambda_1}\left[\left(8\pi+\frac{3}{2}\lambda_2\right)\rho-\frac{1}{2}\lambda_2 p+\frac{5}{2}\lambda_3\rho^2-\frac{3}{2}\lambda_3 p^2-7\lambda_3 p\rho\right] \tag{44}$$

$$\dot{H}_2+H_2^2+\dot{H}_3+H_3^2+H_2H_3=\frac{1}{\lambda_1}\left[-\left(8\pi+\frac{3}{2}\lambda_2\right)p+\frac{1}{2}\lambda_2\rho+\frac{9}{2}\lambda_3 p^2+\frac{1}{2}\lambda_3\rho^2-3\lambda_3 p\rho\right] \tag{45}$$

$$\dot{H}_3+H_3^2+\dot{H}_1+H_1^2+H_3H_1=\frac{1}{\lambda_1}\left[-\left(8\pi+\frac{3}{2}\lambda_2\right)p+\frac{1}{2}\lambda_2\rho+\frac{9}{2}\lambda_3 p^2+\frac{1}{2}\lambda_3\rho^2-3\lambda_3 p\rho\right] \tag{46}$$

$$\dot{H}_1 + H_1^2 + \dot{H}_2 + H_2^2 + H_1H_2 - \frac{l^2}{A^2} = \frac{1}{\lambda_1}\left[-\left(8\pi + \frac{3}{2}\lambda_2\right)p + \frac{1}{2}\lambda_2\rho + \frac{9}{2}\lambda_3 p^2 + \frac{1}{2}\lambda_3\rho^2 - 3\lambda_3 p\rho\right] \tag{47}$$

From equations (44)-(47), we get

$$\begin{aligned} &4\dot{H}_1 + 2\dot{H}_3 + 4H_1^2 + 2H_3^2 \\ &\qquad = \frac{1}{\lambda_1}\left[-\left(8\pi + \frac{3}{2}\lambda_2\right)(3p+\rho) + \frac{1}{2}\lambda_2(p+3\rho) + 15\lambda_3 p^2 - \lambda_3\rho^2 - 2\lambda_3 p\rho\right] \end{aligned} \tag{48}$$

The analysis in the previous sections indicate that our model exhibits characteristics consistent with the quintessence dark energy model. Thus, to investigate the evolution of energy density (ρ) and pressure (p) in our model, over cosmic time t, we adopt the Equation of State parameter $\omega = \frac{p}{\rho}$ within the quintessence regime $-1 < \omega < -\frac{1}{3}$. By analyzing the energy density and pressure in this context, we can further explore the physical implications of the model. Now, considering the equation of state $p = \omega\rho$, from equations (32), (34) and (48), we find

$$\begin{aligned} \rho = \frac{1}{2(5\omega+1)(3\omega-1)\lambda_3}\Bigg[&(8\pi(1+3\omega) + 4\lambda_2\omega) + \Bigg\{(8\pi(1+3\omega) + 4\lambda_2\omega)^2 + \\ &4(5\omega+1)(3\omega-1)\lambda_3\left(\frac{2\lambda_1(\beta^2-\beta)}{t^2} - \frac{4C_0^2k_1\lambda_1 t^{2\beta}}{(\frac{l^2t^2}{1-\beta^2} + C_0^2k_1\beta t^{2\beta})^2(1+\beta)}\left(l^2(2\beta-1) + C_0^2k_1\beta t^{2\beta-2}\right)\right)\Bigg\}^{\frac{1}{2}}\Bigg] \end{aligned} \tag{49}$$

$$\begin{aligned} p = \frac{\omega}{2(5\omega+1)(3\omega-1)\lambda_3}\Bigg[&(8\pi(1+3\omega) + 4\lambda_2\omega) + \Bigg\{(8\pi(1+3\omega) + 4\lambda_2\omega)^2 + \\ &4(5\omega+1)(3\omega-1)\lambda_3\left(\frac{2\lambda_1(\beta^2-\beta)}{t^2} - \frac{4C_0^2k_1\lambda_1 t^{2\beta}}{(\frac{l^2t^2}{1-\beta^2} + C_0^2k_1\beta t^{2\beta})^2(1+\beta)}\left(l^2(2\beta-1) + C_0^2k_1\beta t^{2\beta-2}\right)\right)\Bigg\}^{\frac{1}{2}}\Bigg] \end{aligned} \tag{50}$$

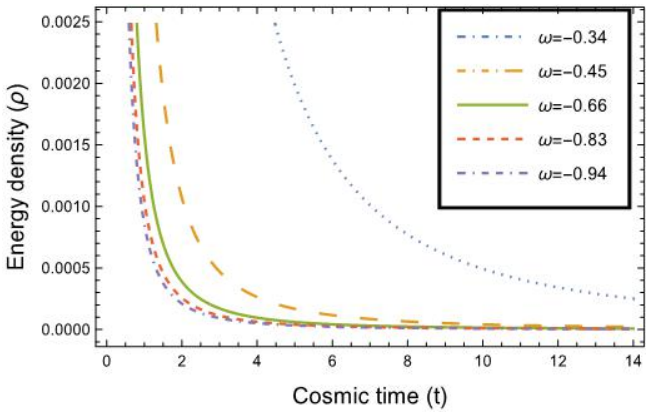

Figure 7. Variation of the energy density ρ v/s cosmic time t

In Figure 7, we present the evolution of the energy density ρ as a function of cosmic time t for different values of the Equation of State parameter viz. $\omega = -0.34, -0.45, -0.66, -0.83, -0.94$ within the quintessence regime. The plot reveals that the energy density starts with significantly large values at the early stages of the universe. As time progresses, ρ decreases steadily, signifying the dilution of energy density due to the universe's expansion.

Figure 8 depicts the evolution of pressure (p) as a function of cosmic time (t). The graph shows that the pressure remains negative throughout the entire evolution, a key characteristic of dark energy. Negative pressure is essential for generating the repulsive gravitational force responsible for the accelerated expansion of the universe. In the early stages of cosmic evolution, the magnitude of the negative pressure is relatively large, corresponding to the dominance of energy components with high density and strong negative pressure, such as quintessence or other dynamic dark energy models. As the universe evolves, the magnitude of p gradually decreases. At late times, the pressure asymptotically approaches

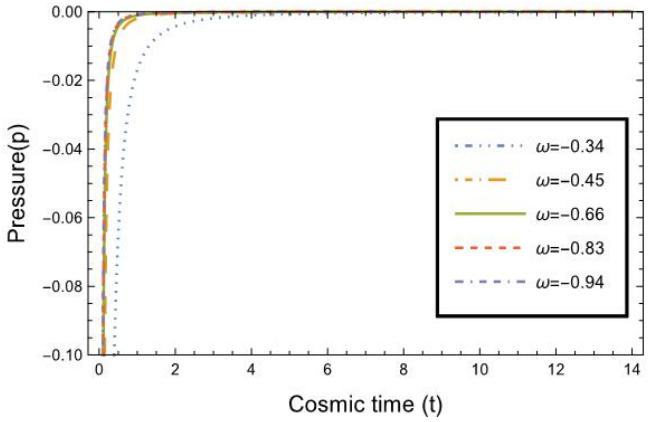

Figure 8. Variation of pressure p v/s cosmic time t with $\omega = -0.34, -0.45, -0.66, -0.83, -0.94$

zero, indicating a transition towards a more stable expansion phase. This behavior is consistent with a dark energy model where the Equation of State parameter (ω) lies in the range $-1 < \omega < -\frac{1}{3}$, as in quintessence. The eventual approach of p to zero suggests that the universe evolves towards a de Sitter like state, characterized by nearly constant energy density and an exponential expansion phase. This result underscores the dynamic nature of the universe's evolution, where negative pressure plays a pivotal role in shaping its expansion history. The gradual reduction in the magnitude of pressure aligns with the transition from a matter dominated phase to an accelerated expansion phase, dominated by dark energy effects.

6. THE FUNCTIONAL $f(R,T)$ OF THE MODEL

From Eq.(10), the trace T of stress-energy tensor T_{ij} is obtained as

$$T = \frac{-1}{2(5\omega+1)\lambda_3}\Bigg[(8\pi(1+3\omega)+4\lambda_2\omega)+ \Bigg\{(8\pi(1+3\omega)+4\lambda_2\omega)^2+4(5\omega+1)(3\omega-1)\lambda_3\left(\frac{2\lambda_1(\beta^2-\beta)}{t^2} - \frac{4C_0^2k_1\lambda_1t^{2\beta}}{(\frac{l^2t^2}{1-\beta^2}+C_0^2k_1\beta t^{2\beta})^2(1+\beta)}\left(l^2(2\beta-1)+C_0^2k_1\beta t^{2\beta-2}\right)\right)\Bigg\}^{\frac{1}{2}}\Bigg] \tag{51}$$

Again, the Ricci scalar R for the metric (14) is obtained as

$$R = -2\left(\frac{\ddot{A}}{A}+\frac{\ddot{B}}{B}+\frac{\ddot{C}}{C}+\frac{\dot{A}}{A}\frac{\dot{B}}{B}+\frac{\dot{B}}{B}\frac{\dot{C}}{C}+\frac{\dot{C}}{C}\frac{\dot{A}}{A}-\frac{l^2}{A^2}\right) \tag{52}$$

For our model, R is obtained as

$$R = \frac{2}{\left(\frac{l^2t^2}{1-\beta^2}+C_0^2k_1t^{2\beta}\right)(1-\beta^2)^2}[l^2(1-\beta^2)^2-l^4(1+\beta+\beta^2)t^2 -2C_0^2k_1(1-\beta^2)(1-2\beta+4\beta^2)t^{2\beta}+3C_0^4k_1^2\beta(1-2\beta)(1-\beta^2)^2t^{4\beta-2}] \tag{53}$$

Therefore, the functional $f(R,T)$ of our model is obtained as

$$
\begin{aligned}
f(R,T) &= f_1(R) + f_2(T) \\
&= \lambda_1 R + \lambda_2 T + \lambda_3 T^2 \\
&= \frac{2\lambda_1}{\left(\frac{l^2t^2}{1-\beta^2} + C_0^2 k_1 t^{2\beta}\right)(1-\beta^2)^2}[l^2(1-\beta^2)^2 - l^4(1+\beta+\beta^2)t^2 \\
&\qquad - 2C_0^2 k_1(1-\beta^2)(1-2\beta+4\beta^2)t^{2\beta} + 3C_0^4 k_1^2 \beta(1-2\beta)(1-\beta^2)^2 t^{4\beta-2}] \\
&\quad - \frac{\lambda_2}{2(5\omega+1)\lambda_3}\Bigg[(8\pi(1+3\omega)+4\lambda_2\omega) + \\
&\Bigg\{(8\pi(1+3\omega)+4\lambda_2\omega)^2 + 4(5\omega+1)(3\omega-1)\lambda_3\Bigg(\frac{2\lambda_1(\beta^2-\beta)}{t^2} \\
&- \frac{4C_0^2 k_1\lambda_1 t^{2\beta}}{(\frac{l^2t^2}{1-\beta^2} + C_0^2 k_1\beta t^{2\beta})^2(1+\beta)}\left(l^2(2\beta-1) + C_0^2 k_1\beta t^{2\beta-2}\right)\Bigg)\Bigg\}^{\frac{1}{2}}\Bigg] \\
&\quad + \frac{1}{4(5\omega+1)^2\lambda_3}\Bigg[(8\pi(1+3\omega)+4\lambda_2\omega) + \\
&\Bigg\{(8\pi(1+3\omega)+4\lambda_2\omega)^2 + 4(5\omega+1)(3\omega-1)\lambda_3\Bigg(\frac{2\lambda_1(\beta^2-\beta)}{t^2} \\
&- \frac{4C_0^2 k_1\lambda_1 t^{2\beta}}{(\frac{l^2t^2}{1-\beta^2} + C_0^2 k_1\beta t^{2\beta})^2(1+\beta)}\left(l^2(2\beta-1) + C_0^2 k_1\beta t^{2\beta-2}\right)\Bigg)\Bigg\}^{\frac{1}{2}}\Bigg]^2
\end{aligned}
\tag{54}
$$

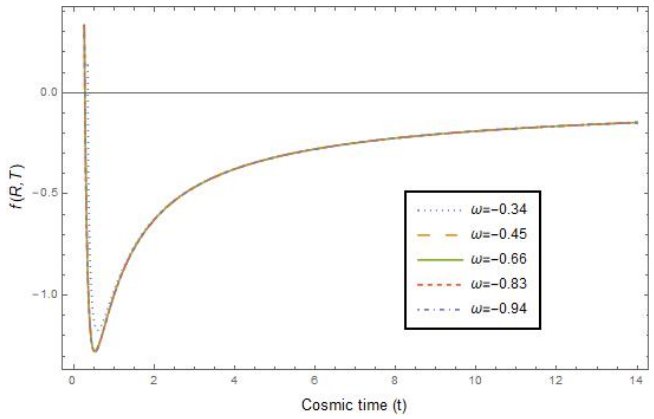

Figure 9. Variation of $f(R,T)$ v/s cosmic time t with $\omega = -0.34, -0.45, -0.66, -0.83, -0.94$

From the graph of $f(R,T)$ versus cosmic time t in figure 9, we see that the functional $f(R,T)$ decreases in the beginning of cosmic evolution but as cosmic time increases, it starts increasing. The graph illustrates the dynamic behavior of the functional $f(R,T)$ throughout the evolution of the universe, revealing a shift in its trend over time.

7. CONCLUSIONS

In this study, we explore a Bianchi type III cosmological model within the framework of $f(R,T)$ gravity, considering the functional form $f(R,T) = f_1(R) + f_2(T)$, where $f_1(R) = \lambda_1 R$, $f_2(T) = \lambda_2 T + \lambda_3 T^2$ and λ_1, λ_2, and λ_3 are free parameters that determine the specific contributions of the Ricci scalar curvature (R) and the trace of the stress-energy tensor (T) to the gravitational dynamics of the model. To solve the gravitational field equations, we assume a power-law expansion, $C = C_0 t^\beta$, where C_0 and β are positive constants. The parameter β is constrained to the range $0 < \beta < 1$, ensuring a physically realistic cosmological model consistent with observed behaviors such as a decelerating phase followed by accelerated expansion.

Exact solutions to the field equations are derived under these assumptions, and the resulting model is analyzed by plotting various parameters of cosmological importance, as functions of cosmic time t. The horizontal axis of the plots is expressed in Gigayears (Gyr), where 1 Gyr corresponds to 10^9 years, to provide a clear representation of the universe's evolution over time.

By varying the parameter β, we examine how the model's qualitative behavior changes with different expansion rates. The plots offer insights into the dynamical properties of the universe, such as its anisotropy, the transition from deceleration to acceleration, and the roles of curvature in driving its evolution. This approach allows us to better understand the implications of $f(R,T)$ gravity and the viability of the chosen functional form in describing the observed universe.

From the variations of cosmologically significant parameters, we observe that volume (V) of the universe increases with cosmic time t which indicates the expansion of the universe. Our model remains anisotropic throughout its evolution. The average Hubble parameter (H) starts at a very high value and decreases over time. The deceleration parameter (q) transits from an early decelerating phase to a late-time accelerating phase, indicating that the universe undergoes accelerated expansion at later times. The jerk parameter (j) decreases with cosmic time t and remains below 1 throughout the universe's evolution, suggesting that our model behaves like a quintessence model of dark energy.

Moreover, the present-day value of the statefinder pair $\{r, s\}$ for our model is found to be in the range $r < 1, s > 0$. For example, with values of the constants $\beta = 0.75$, $k_1 = 0.1$, $C_0 = 1$, $l = 1$, $\lambda_1 = -0.1$, $\lambda_2 = 0.2$, $\lambda_3 = 0.3$, $t = 14$, the present value of the statefinder pair is $\{0.031, 0.126\}$, indicating that the model resembles a quintessence model both in the present and at late times. The statefinder diagnostic provides a deeper insight into the nature of dark energy, with our model's parameters indicating a close resemblance to quintessence, a widely studied candidate for dark energy.

The energy density (ρ) of our model monotonically decreases from a very high initial value to a constant value at late times, while the pressure (p) remains negative throughout its evolution. We also evaluate the Ricci scalar R and the trace T of the stress-energy tensor to determine the functional form $f(R,T)$ of our model. At the early stages of cosmic evolution, the functional $f(R,T)$ exhibits a decreasing pattern. This behavior is primarily driven by the dominance of high curvature (R) and significant contributions from the trace of the stress-energy tensor (T), which characterize the high-energy, dense state of the early universe. During this phase, the rapid expansion and changes in matter-energy densities lead to a reduction in $f(R,T)$. As cosmic time progresses, the functional $f(R,T)$ transitions from a decreasing to an increasing trend. This shift occurs as the influence of matter and radiation diminishes with the universe's expansion. The curvature (R) also evolves due to the decelerating expansion in earlier phases and the subsequent transition to accelerated expansion. The increasing trend of $f(R,T)$ during intermediate times reflects the growing influence of dark energy or the modified gravity terms associated with $f(R,T)$ in shaping the universe's dynamics. This turning point in the behavior of $f(R,T)$ signifies the interplay between the curvature scalar (R) and the trace of the stress-energy tensor (T) as the dominant components of the universe's energy content evolve. The rise in $f(R,T)$ suggests that the modified gravity effects encoded in $f(R,T)$ become increasingly significant as the universe transitions toward its accelerated expansion phase. Overall, the evolution of $f(R,T)$ highlights the adaptability of the $f(R,T)$ framework in capturing the changing dynamics of the universe, from a matter-dominated phase to one governed by dark energy or other modified gravity effects.

In addition to the quantitative analysis, we also discuss the physical implications of our findings in the broader context of cosmological models. The persistent anisotropy in our model suggests that early universe anisotropies can have long-lasting effects, influencing the current and future dynamics of cosmic expansion. The transition of the deceleration parameter from positive to negative values supports the hypothesis that the universe has transitioned from a matter-dominated decelerating phase to a dark energy-dominated accelerating phase.

Acknowledgments

The authors express their profound gratitude to the esteemed referee for his/her valuable comments and suggestions which helped to improve the quality of this paper in the present form.

ORCID

Chandra Rekha Mahanta, https://orcid.org/0000-0002-8019-8824; **Kankana Pathak**, https://orcid.org/0009-0004-0353-809X

REFERENCES

[1] S. Perlmutter, G. Aldering, G. Goldhaber, *et al*. "Measurements of Ω and Λ from 42 high-redshift supernovae," Astrophys. ApJ, **517**, (565) (1999). https://doi.org/10.1086/307221

[2] A. G. Riess, A. V. Filippenko, P. Challis, *et al*. "Observational evidence from supernovae for an accelerating universe and a cosmological constant," The Astronomical Journal, **116** (1009) (1998). https://doi.org/10.1086/300499

[3] R. R. Caldwell, M. Doran, "Cosmic microwave background and supernova constraints on quintessence: Concordance regions and target models," Phys. Rev. D, **69**, 103517 (2004). https://doi.org/10.1103/PhysRevD.69.103517

[4] Zhuo-Yi Huang, B. Wang, E. Abdalla, R.−K, Su, "Holographic explanation of wide-angle power correlation suppression in the Cosmic Microwave Background Radiation," J. Cosmol. Astropart. Phys. **5**, (013) (2006). https://doi.org/10.1088/1475-7516/2006/05/013

[5] K. Land and J. Magueijo, "Examination of Evidence for a preferred Axis in the Cosmic Radiation Anisotropy," Phys. Rev. Lett. **95**, 071301 (2005). https://doi.org/10.1103/PhysRevLett.95.071301

[6] C. L. Bennett, M. Halpern, G. Hinshaw, *et al*. "First-Year Wilkinson Microwave Anisotropy Probe (WMAP)* Observations: Preliminary Maps and Basic Results," Astrophys. J. Suppl. **148**, (1) (2003). https://doi.org/10.1086/377253

[7] C. L. Bennett, D. Larson, J. L. Weiland, *et al*. "Nine-Year Wilkinson Microwave Anisotropy Probe (WMAP) Observations: Final Maps and Results," ApJS, **208**, 20 (2013). https://doi.org/10.1088/0067-0049/208/2/20

[8] D. N. Spergel, L. Verde, H. V. Peiris, *et al*. "First Year Wilkinson Microwave Anisotropy Probe (WMAP) Observations: determination of cosmological parameters," ApJS, **148**, (175) (2003). https://doi.org/10.1086/377226

[9] D. N. Spergel, R. Bean, O. Dor'e, *et al*. "Three-year Wilkinson Microwave Anisotropy Probe (WMAP) observations: implications for cosmology," ApJS, **170**, 377 (2007). https://doi.org/10.1086/513700

[10] M. Tegmark, M. A. Strauss, M. R. Blanton, *et al*. "Cosmological parameters from SDSS and WMAP," Phys. Rev. D, **69**, 103501 (2004). https://doi.org/10.1103/PhysRevD.69.103501

[11] L. Anderson, E. Aubourg, S. Bailey, D. Bizyaev, M. Blanton, A. S. Bolton, *et al*. "The clustering of galaxies in the SDSS-III Baryon Oscillation Spectroscopic Survey: baryon acoustic oscillations in the Data Release 9 spectroscopic galaxy sample," Monthly Notices of the Royal Astronomical Society, **427**(4), 3435-3467 (2012). https://doi.org/10.1093/mnras/stu523

[12] C. Blake, E. A. Kazin, F. Beutler, T. M. Davis, D. Parkinson, S. Brough, *et al*. "The WiggleZ Dark Energy Survey: mapping the distance-redshift relation with baryon acoustic oscillations," Monthly Notices of the Royal Astronomical Society, **418**(3), 1707-1724 (2011). https://doi.org/10.1111/j.1365-2966.2011.19592.x

[13] N. Padmanabhan, X. Xu, D. J. Eisenstein, R. Scalzo, A. J. Cuesta, K. T. Mehta, E. Kazin, "A 2 per cent distance to $z = 0.35$ by reconstructing baryon acoustic oscillations-I. Methods and application to the Sloan Digital Sky Survey," Monthly Notices of the Royal Astronomical Society, **427**(3), 2132-2145 (2012). https://doi.org/10.1111/j.1365-2966.2012.21888.x

[14] T. Barreiro, E. J. Copeland and N. J. Nunes, "Quintessence arising from exponential potentials," Phys. Rev. D. **61**, 127301 (2000). https://doi.org/10.1103/PhysRevD.61.127301

[15] T. Chiba, T. Okabe, M. Yamaguchi, "Kinetically driven quintessence," Phys. Rev. D, **62**, 023511 (2000). https://doi.org/10.1103/PhysRevD.62.023511

[16] T. Padmanabhan, "Accelerated expansion of the universe driven by tachyonic matter,"Phys. Rev. D, **66**, 021301 (2002). https://doi.org/10.1103/PhysRevD.66.021301

[17] R. R. Caldwell, M. Kamionkowski and N. N. Weinberg, "Phantom Energy: Dark Energy with $\omega <$-1 Causes a Cosmic Doomsday," Phys. Rev. Lett. **91**, 071301 (2003). https://doi.org/10.1103/PhysRevLett.91.071301

[18] M. Li, "A model of holographic dark energy,"Phys. Lett. B, **603**, 1 (2004), https://doi.org/10.1016/j.physletb.2004.10.014

[19] C. Tsallis, and L. J. L. Cirto, "Black hole thermodynamical entropy," Eur. Phys. J. C, **73**, 2487 (2013), https://doi.org/10.1140/epjc/s10052-013-2487-6

[20] D. J. Barrow, "The area of a rough black hole," Phys. Lett. B, **808**, 135643 (2020). https://doi.org/10.1016/j.physletb.2020.135643

[21] A. Kamenshchik, U. Moschella, V. Pasquier, "An alternative to quintessence," Phys. Lett. B, **511**, 265-268 (2001). https://doi.org/10.1016/S0370-2693(01)00571-8

[22] M. C. Bento, O. Bertolami, and A. A. Sen, "Generalized Chaplygin gas, accelerated expansion, and dark-energy-matter unification," Phys. Rev. D, **66**, 043507 (2002). https://doi.org/10.1103/PhysRevD.66.043507

[23] H. B. Benaoum, "Modified Chaplygin Gas Cosmology," Advances in High Energy Physics, **2012**, 357802 (2012). https://doi.org/10.1155/2012/357802

[24] S. M. Carroll, V. Duvvuri, M. Trodden, and M. S. Turner, "Is cosmic speed-up due to new gravitational physics?" Phys. Rev. D, **70**, 043528 (2004). https://doi.org/10.1103/PhysRevD.70.043528

[25] T. Harko, F. S. N. Lobo, S. Nojiri and S. D. Odintsov, "$f(R,T)$ gravity," Phys. Rev. D, **84**, 024020 (2011). https://doi.org/10.1103/PhysRevD.84.024020

[26] S. M. Carroll, A. D. Felice, V. Duvvuri, D. A. Easson, M. Trodden, and M. S. Turner, "Cosmology of generalized modified gravity models," Phys. Rev. D, **71**, 063513 (2005). https://doi.org/10.1103/PhysRevD.71.063513

[27] R. Ferraro, and F. Fiorini, "Modified teleparallel gravity: Inflation without an inflaton," Phys. Rev. D, **75**, 084031 (2007). https://doi.org/10.1103/PhysRevD.75.084031

[28] J. B. Jiménez, L. Heisenberg, and T. Koivisto, "Coincident general relativity," Phys. Rev. D, **98**(4), 044048 (2018). https://doi.org/10.1103/PhysRevD.98.044048

[29] M.J.S. Houndjo, "Reconstruction of $f(R,T)$ gravity describing matter dominated and accelerated phases," Int. J. Mod. Phys. D, **21**, 1250003-1250016 (2012). https://doi.org/10.1142/S0218271812500034

[30] P. K. Sahoo, S. K. Sahu, and A. Nath, "Anisotropic Bianchi-III cosmological model in $f(R,T)$ gravity," Eur. Phys. J. Plus, **131**, 18 (2016). https://doi.org/10.1140/epjp/i2016-16018-6

[31] G. C. Samanta, and B. K. Bishi, "Geometry of the Universe Described by Wet Dark Fluid in $f(R,T)$ Theory of Gravity," Iran. J. Sci. Technol. Trans. A Sci. **41**, 223 (2017). https://doi.org/10.1007/s40995-017-0215-z

[32] S. Arora, S. Bhattacharjee, and P. K. Sahoo, "Late-time viscous cosmology in $f(R,T)$ gravity," New Astronomy, **82**, 101452 (2021). https://doi.org/10.1016/j.newast.2020.101452

[33] C. R. Mahanta, S. Deka, and K. Pathak, "Anisotropic Cosmological Model in $f(R,T)$ Theory of Gravity with a Quadratic Function of T," East European Journal of Physics, (3), 43-52 (2023). https://doi.org/10.26565/2312-4334-2023-3-02

[34] C. R. Mahanta, K. Pathak, and D. Das, "FLRW Cosmological Model with Quadratic Functional Form in $f(R,T)$ Theory of Gravity," East European Journal of Physics, (1), 29-43 (2025). https://doi.org/10.26565/2312-4334-2025-1-03

[35] M. K. Verma, M. K. Singh, and S. Ram, "Anisotropic Bulk Viscous Fluid Cosmological Model with Zero-Rest-Mass Scalar Field and Time-Dependent Cosmological Term," Int. J. Theor. Phys. **51**, 1729-1736 (2012). https://doi.org/10.1007/s10773-011-1050-1

[36] D. R. K. Reddy, R. Santikumar, and R. L. Naidu, "Bianchi type-III cosmological model in $f(R,T)$ theory of gravity," Astrophys. Space Sci. **342**, 249-252 (2012). https://doi.org/10.1007/s10509-012-1158-7

[37] V. Sahni, *et al.*, "Statefinder - a new geometrical diagnostic of dark energy," JETP Lett. **77**, 201 (2003). https://doi.org/10.1134/1.1574831

ДОСЛІДЖЕННЯ ВСЕСВІТУ БІАНКІ III ТИПУ З КВАДРАТИЧНИМ СЛІДОМ ТЕНЗОРА ЕНЕРГІЇ-НАПРУЖЕННЯ В $f(R,T)$ ТЕОРІЇ ГРАВІТАЦІЇ

Чандра Рекха Маханта, **Канкана Патхак**

Кафедра математики, Університет Гаухаті, Гувахаті - 781014, Індія

У цій роботі ми розглядаємо просторово однорідний та анізотропний всесвіт Біанкі III типу в гравітації $f(R,T)$ з функціональною формою $f(R,T) = f_1(R) + f_2(T)$ з $f_1(R) = \lambda_1 R$ та $f_2(T) = \lambda_2 T + \lambda_3 T^2$, де λ_1, λ_2 та λ_3 – вільні параметри. Ми отримуємо точні розв'язки рівнянь гравітаційного поля, розглядаючи степеневий розклад коефіцієнта масштабування напрямку. Контролюючи поточні значення параметрів космологічного значення, таких як параметр Хаббла H та параметр уповільнення q, досліджується динаміка та фізичні характеристики моделі. Ми також визначаємо функціональну форму $f(R,T)$ нашої моделі, оцінюючи скаляр Річчі R та слід T тензора енергії-напруження. Ми виявляємо, що наша модель залишається анізотропною протягом усієї своєї еволюції, а тиск космічної матерії залишається негативним. Виявлено, що параметр рівняння стану ω лежить у режимі квінтесенції, і тому наша модель поводиться як модель квінтесенції темної енергії.

Ключові слова: *простір-час типу III Біанкі; $f(R,T)$ гравітація; параметр уповільнення; параметр Хаббла*